Biochemistry

 Volume 40, Number 11 March 20, 2001

Current Topics

The Ribosome at Atomic Resolution†

Peter B. Moore*

Departments of Chemistry and of Molecular Biophysics and Biochemistry, Yale University, New Haven, Connecticut 06520

Received December 27, 2000; Revised Manuscript Received January 24, 2001

ABSTRACT: The publication of atomic resolution crystal structures for the large ribosomal subunit from *Haloarcula marismortui* and the small ribosomal subunit from *Thermus thermophilus* has permanently altered the way protein synthesis is conceptualized and experiments designed to address its unresolved issues. The impact of these structures on RNA biochemistry is certain to be no less profound. The background and substance of these developments are reviewed here.

The ribosome crystal structures published last year are the culmination of decades of effort on the part of the entire scientific community concerned with ribosomes. It is appropriate therefore to begin by reminding the reader of the biochemical and crystallographic background of the field. Those interested in a more comprehensive overview should consult a recently published symposium volume (*1*).

Biochemical Background. The cellular components called ribosomes were discovered in the 1950s as a result of biochemical studies of protein synthesis and investigations of cellular structure done by fractionation methods and electron microscopy (*2*). By 1960, it was evident that all cells capable of synthesizing protein contain ribosomes and that ribosomes catalyze protein synthesis. The substrates of ribosomes are aminoacyl tRNAs,[1] and the sequences of their polypeptide products are determined by the interactions they mediate between aminoacyl tRNAs and messenger RNA templates.

Ribosomes have diameters of about 250 Å and are roughly two-thirds RNA and one-third protein. While there is species-to-species variation in ribosome size and protein/RNA ratio, they all have two subunits, one about twice the mass of the other. In prokaryotes, the small (30S) subunit consists of a single RNA about 1500 nucleotides long (16S rRNA) and single copies of each of about 20 different protein molecules (*3*). The large (50S) subunit contains an RNA of about 2900 nucleotides (23S rRNA), an RNA of about 120 nucleotides (5S rRNA), and single copies of each of roughly 30 different proteins. One large subunit protein is present in 4 copies. The typical prokaryotic ribosome has a molecular weight around 2.5×10^6 and sediments at 70S. Eukaryotic ribosomes are larger than prokaryotic ribosomes because they have more components and because their components are bigger, on average, but their architecture is fundamentally the same.

For more than a quarter of a century, a fundamental objective of those interested in the ribosome has been to explain its protein synthetic activity in atomic detail, and almost all the issues that need addressing are manifest in the elongation phase of protein synthesis, i.e., the phase during which nascent polypeptides are extended by the addition of amino acids at their C-termini. The standard description of elongation posits a ribosome that has three distinct tRNA binding sites: an A site, a P site, and an E site. Since the anticodon stem/loops of tRNAs interact primarily with the small subunit and the CCA terminus of

† This work was supported by grants from NIH (GM54216) and the Agouron Institute.

* To whom correspondence should be addressed.

[1] Abbreviations: DMS, dimethyl sulfate; EF-G, elongation factor G; EF-Tu, elongation factor Tu; EF-1α, elongation factor 1α; EF-2, elongation factor 2; mRNA, messenger RNA; rRNA, ribosomal RNA; tRNA, transfer RNA.

10.1021/bi0029402 CCC: $20.00
Published on Web 02/20/2001

their acceptor stems interacts exclusively with the large subunit, there are A, P, and E sites on *both* subunits (*4*).

At the beginning of each cycle of elongation, either an aminoacylated initiator tRNA or a peptidyl tRNA occupies the P site of both subunits, and its anticodon is base-paired with the mRNA codon presented there. On the small subunit, the P and A sites are juxtaposed so that the mRNA triplet 3′ to the triplet in the P site will interact with the anticodon of a tRNA bound to the A site. In the first step of the cycle, an aminoacylated tRNA is selected from the cellular pool that has an anticodon sequence complementary to the A-site triplet. It is delivered to the A site of both subunits by a protein called EF-Tu in prokaryotes (EF-1α in eukaryotes), and the specificity of its selection is enhanced by proofreading.

Once a cognate aminoacyl tRNA enters the A site, the second step of the cycle occurs: peptide bond formation. The amino acid or peptide esterified to the CCA end of the tRNA in the P site is transferred to the α-amino group of the amino acid esterified to the CCA sequence of the tRNA in the A site, which lengthens the nascent peptide chain by one residue. The enzymatic activity responsible is called peptidyl transferase and is intrinsic to the large ribosomal subunit. Peptide bond formation is accompanied by a shift of the acceptor end of the newly deacylated tRNA from the 50S P site to the 50S E site, and at the same time, the acceptor end of the tRNA carrying the nascent polypeptide moves from the 50S A site to the 50S P site. Since the anticodon ends of both tRNAs remain fixed on the small subunit, the resulting tRNA configurations are called "hybrid states" (*4*).

In the last step of the elongation cycle, translocation, the system is reinitialized. With the assistance of a protein factor called EF-G (prokaryotes) or EF-2 (eukaryotes), the peptidyl tRNA is relocated so that it occupies the P site on both subunits, the deacylated tRNA moves entirely into the E site preparatory to its dissociation from the ribosome, and the mRNA advances on the ribosome by three nucleotides in the 5′ direction. The product of translocation can thus engage in another round of elongation.

Crystallographic Background. It has always been obvious that an atomic resolution, three-dimensional structure of the ribosome—any ribosome—would have an enormous impact on our understanding of protein synthesis and that X-ray crystallography was the only technique likely to yield that information. Consequently, by the early 1960s efforts to crystallize ribosomes were already underway (A. Rich, personal communication), and by the mid-1960s, tissues had been discovered in which microscopic, two-dimensional ribosome crystals appear spontaneously (*5*), suggesting that the quest for three-dimensional crystals was not as quixotic as it must sometimes have seemed (see refs *6* and *7*). Nevertheless, it was not until 1980 that the first macroscopic, three-dimensional crystals were reported (*8*). They were the product of a crystallization initiative organized in Berlin at the Max Planck Institute by H. G. Wittmann and Ada Yonath. The first crystals diffracted poorly, but their existence encouraged the search for better ones.

Crystallization studies continued throughout the 1980s, both in Berlin and in the Soviet Union, where a group at Pushchino first demonstrated the crystallization of 70S ribosomes and 30S subunits from *Thermus thermophilus* (*9*). By the end of the decade, the list of bacterial ribosomes and ribosomal subunits known to crystallize had become quite long (*10*), and the most promising crystals appeared to be those of the large ribosomal subunit from *Haloarcula marismortui*, which had been shown to diffract beyond 3 Å resolution (*11*, *12*).

Data Collection and Processing. Even if the crystals obtained in 1980 had been as good as those available today, it would have been years before their structures were solved. The collection and analysis of the diffraction data from such crystals posed challenges that could not have been met in 1980; ribosomes were too big. Even by today's standards, ribosomes are impressive; the molecular weight of the small subunit is more than twice that of the largest, asymmetric structure solved at atomic resolution prior to 2000, and the large subunit is twice as big again as that.

The bigger the molecule, the larger the size of the diffraction data sets that have to be collected and processed to solve their structures. Furthermore, the bigger the molecule, the weaker its crystals diffract X-rays, and weak diffraction patterns are hard to measure with the requisite accuracy. Only recently have computers and computer codes become available that can deal with ribosome-size data sets, and only with the development of synchrotron light sources did X-ray beams become available that are bright enough to make high-resolution data collection from ribosome crystals practical.

Synchrotron radiation was not the whole answer to the data collection problem, however. X-rays are ionizing radiation, and the chemical damage they cause destroys crystal diffraction patterns. There are limits, therefore, to how much information can be squeezed out of a weakly diffracting crystal by increasing the X-ray dose to which it is exposed. The limitation imposed by radiation damage were surmounted in two ways. First, the damage X-rays do to diffraction patterns can be reduced dramatically by freezing crystals prior to data collection, which reduces the diffusion of the reactive species generated by ionizations. Its effectiveness was first demonstrated for ribosome crystals by Yonath and co-workers (*13*). Second, imaging plate and charge-coupled device area detectors were devised that make it possible to detect *all* the photons a crystal diffracts with quantum efficiencies approaching 1.0, which minimizes the X-ray dose crystals must be exposed to during data collection.

Phasing Ribosomal Diffraction Patterns. By 1990, good ribosome crystals existed, and the techniques and instruments available for data collection and processing were adequate. The problem that remained was the one that had challenged Kendrew and Perutz 40 years earlier: phasing (see ref *14*). Their solution to the phase problem, multiple isomorphous replacement, is hard to apply to crystals of big, asymmetric molecules such as the ribosome. Large numbers of heavy (i.e., high atomic number) atoms must be bound in each unit cell to alter diffraction intensities significantly, but the methods used to extract heavy atom positions from macromolecular diffraction data become problematic when the numbers to be located are large, and phase information cannot be obtained if their positions are not determined. (Phasing methods based on anomalous scattering suffer the same limitation.)

The phase problem was first solved for ribosome crystals by the group working at Yale on crystals of the 50S subunit

from *H. marismortui* (*15*). Their strategy depended on solving the phase problem first at low resolution by methods that work well at low resolution and then using the resulting low-resolution phases to solve the phase problem again at high resolution by standard isomorphous replacement techniques. Success with the first step all but guarantees the success of the second because once low-resolution phases are in hand, heavy atom positions can be determined by techniques that are insensitive to the number of heavy atoms present.

The two approaches the Yale group used for low-resolution phasing had both been employed previously in other contexts. First, isomorphous replacement was done with cluster compounds that contain many heavy atoms instead of the compounds more commonly used, which contain only one or a few heavy atoms, (e.g., refs *16* and *17*). Diffraction intensities may change significantly when only small numbers of cluster molecules bind per macromolecule because each contains many heavy atoms. Furthermore, at low resolution, all of the heavy atoms in a cluster contribute to a crystal's diffraction pattern as though they were in the same place. Thus, at low resolution, the number of different heavy atom positions to be determined can be small enough so that standard methods will find them. Second, phases were obtained by molecular replacement using three-dimensional, electron microscopic images of the ribosome (e.g., ref *18*). This approach was particularly attractive because the techniques that had just been developed for reconstructing three-dimensional images of particulate objects from electron micrographs of randomly oriented single particles can yield ribosome images that are remarkable both for their accuracy and for their resolution (*19*, *20*).

After overcoming a serious crystal polymorphism problem (see ref *21*), in 1998, with the collaboration of Joachim Frank and co-workers, the Yale group obtained a 9 Å resolution electron density map of the *H. marismortui* 50S subunit. The phases for this map were determined using both cluster compound, isomorphous replacement data and molecular replacement information obtained using a 20 Å resolution reconstruction of the *H. marismortui* large subunit (*15*). In the summer of 1999, a 5.0 Å resolution version of the same electron density map was published (*21*), and simultaneously, the group at the MRC led by Ramakrishnan announced a 5.5 Å electron density map for the *T. thermophilus* small subunit that had been phased at low resolution using cluster compounds (*22*). In the autumn of 1999, Noller's group at Santa Cruz presented their 7.8 Å resolution electron density map of the 70S ribosome from *T. thermophilus*, the initial, low-resolution phases for which were obtained by electron microscopy/molecular replacement (*23*). Finally, at the end of 1999, the Max Planck group announced a cluster compound-derived, 4.5 Å resolution electron density map of the *T. thermophilus* small subunit obtained from crystals identical to those being studied at the MRC but less fully interpreted (*24*).

The struggle to reach atomic resolution ended the following year. The Yale map of the large subunit had attained a resolution of 2.4 Å, and full RNA coordinates and protein backbone coordinates were published for the 90% of the large subunit that is well enough ordered to be modeled (*25*). The resolution of the MRC small subunit electron density map had improved to 3.0 Å, and backbone and side chain coordinates were presented for both protein and RNA that are complete to the extent disorder allows (~98%) (*26*). The resolution of the Max Planck map of the small subunit had reached 3.3 Å, which is sufficient for the interpretation of well-ordered RNA density but problematic for the interpretation of protein density (*27*). The structure published by the Max Planck group, which includes about 70% of the atoms in the subunit, is similar to that of the MRC group.

The Santa Cruz group has not yet published a higher resolution version of their 70S structure but will probably do so soon. The Santa Cruz structure is of the utmost interest because the ribosomes in their crystals have both messenger RNA and tRNAs bound. Thus their structure will provide additional information about the ribosome in one of its functional states. The functional relevance of the structures now available for the two subunits is less obvious. The crystals in question diffract to about 5 Å resolution, which means that an independently determined, atomic resolution structure will not emerge, but a lot will be learned because the high-resolution structures for the two subunits can be used to help with interpretation.

Generalities about Ribosome Architecture. The structures of the two subunits are a stunning validation of the phylogenetic method for determining RNA secondary structure (*28*). The overwhelming majority of the stem/loop structures identified phylogenetically exist in the ribosome. As expected, its "failures" are largely failures of omission, i.e., helices predicted to be shorter than they really are or sequences identified as unstructured that are structured. The number of secondary structure elements predicted that do not exist is very small.

Only a few new RNA secondary structure motifs are going to emerge from these structures. Given that the amount of high-resolution RNA structure available for inspection increased roughly 10-fold when the structures of the ribosomal subunits were published, this finding may seem surprising. However, it was clear before these structures appeared that most of the commonly encountered RNA motifs had already been discovered (*29*). The universe of RNA secondary structure motifs is small.

What will result from these structures is a major improvement in our understanding of RNA tertiary structure. Little was known about RNA tertiary structure prior to 2000 because most of the RNAs whose structures were known at atomic resolution are too small to have any. It will take a while to harvest all the tertiary information there structures contain, but one new tertiary motif has already emerged. In many places in both subunits, tertiary structure is stabilized by interactions involving short runs of stacked As that have their minor groove edges inserted into the minor groove edge of base pairs that are components of helices (*25*, *26*).

The structures of the two subunits also have much to teach about the way proteins stabilize RNA structure. In the past, for understandable reasons, biochemists interested in rRNA/ribosomal protein interactions focused on the strongest interaction each protein makes with rRNA. This has inadvertently fostered the impression that the typical ribosomal protein only has one or, at most, two significant rRNA binding sites. In fact, most ribosomal proteins have many rRNA binding sites, and they enable these proteins to stabilize rRNA tertiary structure by cross-linking. RNA

structure stabilization appears to be the primary function of most ribosomal proteins.

Many ribosomal proteins have globular domains from which polypeptide tails extend that have little or no secondary structure. A few have no globular domains at all; they are all tail. The tails of these proteins are all strongly basic and insert into crevices between rRNA helices in subunit interiors. The intimacy of the mixture of RNA and protein that results implies that ribosome assembly in vivo must be a controlled, ordered process, and about this aspect of ribosome biochemistry little is known. Whether they have tails or not, the globular domains of ribosomal proteins are all found exposed on the surfaces of their respective subunits. However, the concentration of protein domains on the surface of each subunit that interacts with the other subunit is low.

The relationship between subunit morphology and rRNA domain structure differs in the two subunits. The small subunit has three morphological domains—its head, body, and platform—and its rRNA, 16S rRNA, has three secondary structure domains, each of which forms the bulk of a single morphological domain. Including 5S rRNA, there are seven secondary structure domains in the rRNAs of the large subunit, but morphologically, the large subunit is a monolithic, single-domain structure. When thinking about these observations, it is important to remember that the domain structures of proteins are mandated by the mixed hydrophobic/hydrophilic character of their polypeptide chains. There is no corresponding physicochemical reason why a globular RNA, which is an assembly of helical rods that all have hydrophilic surfaces, must have morphological domains. The domains of the small subunit must exist for functional reasons.

Small Subunit Function. The primary function of the small ribosomal subunit is mediation of the interactions between mRNAs and tRNAs on which the fidelity of translation depends. It is gratifying, therefore, that the small subunit structures just published provide a great deal of information about tRNA interactions. The small subunit includes a protruding RNA stem/loop, often called the "spur", that resembles the anticodon stem/loop of a tRNA in structure. In the crystals studied by the MRC and Max Planck groups subunits are packed so that the spur from one subunit inserts into the P site of its neighbor, where its "anticodon loop" interacts with a flexible segment of the 3′ end of 16S rRNA, which happens to occupy the mRNA binding region of the P site (*27*, *30*). When it rains, it pours!

The identification of the spur interaction with the P-site tRNA/mRNA interaction is strongly supported by the observation that when the structure of the isolated small subunit is superimposed on the small subunit region of the 7.8 Å resolution electron density map of the 70S ribosome, which includes bound tRNAs (*23*), the spur aligns with the anticodon stem/loop of the tRNA in the 70S P site. This superposition also shows how tRNAs bound to the A site and the E site interact with the small subunit and how mRNAs bind to the small subunit. However, helpful as this information is, it is unlikely to lead directly to a full understanding of fidelity. Discrimination between noncognate and near-cognate tRNAs depends on interactions involving elongation factors and the large subunit, as well as the small subunit.

In its first series of papers, the MRC group published the structure of the small ribosomal subunit with the antibiotics spectinomyin, streptomycin, and paromomycin all bound to it simultaneously (*30*). This experiment worked because the sites to which these antibiotics bind do not overlap. Spectinomyin binds to a site composed entirely of RNA and appears to prevent small subunit motions essential for the translocation step of elongation. The streptomycin site contains both protein and RNA, but streptomycin too appears to interfere with a small subunit conformation transition, in this case one that controls the accuracy of decoding. The last of the trio, paromomycin, binds to an all-RNA site close to the place where A-site codon/anticodon interactions occur on the small subunit. Its presence influences the positions of two adenines that may be involved in interactions that enable the ribosome to determine whether the interaction between an A-site codon and the anticodon of an incoming tRNA is cognate or not.

Subsequently, the MRC group provided structures for the small subunit with three more antibiotics bound: tetracycline, pactamycin, and hygromycin B (*31*). Tetracyline, it turns out, binds to two sites, both composed entirely of RNA, one of which is close enough to the A site to account for the drug's well-known activity as an inhibitor of A-site tRNA binding. Its second binding site is close to H27, where a conformational switch is known to occur during protein synthesis that affects the fidelity of decoding. The binding of tetraclycline to that site may also be significant physiologically. Pactamyin, which has long been thought to be an initiation inhibitor, binds to another all-RNA site where it may prevent a conformational change important for initiation, and hygromycin B, which inhibits translocation by fixing tRNAs in the A site, binds close to helix 44, which is believed to move during translocation.

Large Subunit Function: Puromycin and Peptide Transfer. The large subunit contributes to elongation by promoting both factor binding and peptide transfer. Its structure has relatively little to tell us about the former because both subunits are affected when factors bind. On the topic of peptide transfer, on the other hand, the structure of the large subunit is quite informative. On the face of it, peptide transfer is the simplest of ribosome functions. All the peptidyl transferase site must do is mediate the nucleophilic attack of an α-amino group of an amino acid on the carbonyl carbon of ester, and the site is entirely contained in the large subunit.

Most of what is known about peptide transfer has been learned using puromycin, which is an antibiotic consisting of a modified tyrosine linked by an amide bond to the ribose of a modified adenosine (Figure 1A). Puromycin's similarity to the A-amino acid part the -CCA-amino acid sequence of aminoacylated tRNAs is obvious, and happily for biochemists both 70S ribosomes and 50S subunits catalyze the transfer of peptides from P-site-bound peptidyl tRNAs to the α-amino group of puromycin (*32*). The large subunit catalyzes an even simpler version of the same reaction: the transfer of formylmethionine from CCA-formylmethionine to puromycin (*33*). This so-called fragment reaction is relevant here because analogues of its substrates have been used by the Yale group to study the peptidyl transferase site crystallographically (*34*).

Useful as it is, the fragment reaction has two properties that suggest it may not fully capture what occurs in the

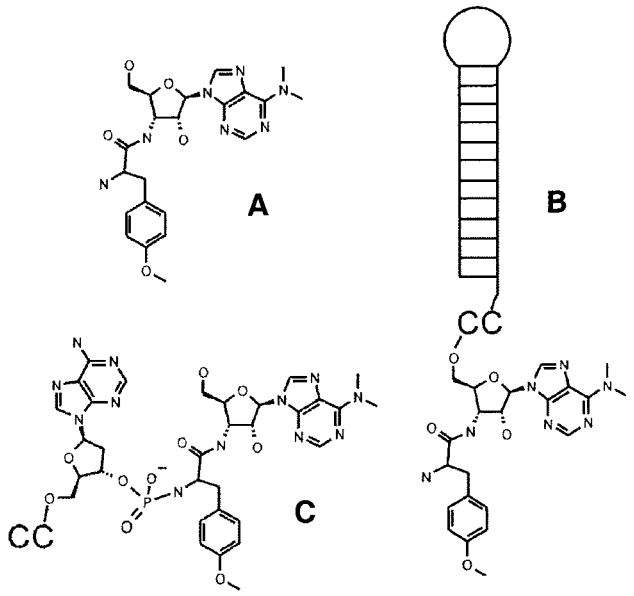

FIGURE 1: Petidyl transferase analogues. (A) Puromycin. (B) An A-site substrate analogue. The stem of the stem/loop shown schematically has the same sequence as the acceptor stem of tyrosyl tRNA, and its loop is a GNRA tetaloop. (C) The transition state analogue, CCdA-P-puro, often referred to as the Yarus inhibitor (*38*). (Figure adapted from ref *33*.)

peptidyl transferase site during protein synthesis. The more obvious of the two is its requirement for substantial concentrations of methanol or ethanol, but this is probably less important than it may seem. Substrates only slightly more elaborate than the standard ones react on the large subunit in the absence of alcohol (S. Strobel, personal communication). Less obvious, but far more troubling, the fragment reaction is very slow. In bacteria such as *Escherichia coli* (*35*) and in well-tuned in vitro systems derived from them (e.g., refs *36* and *37*) amino acids are added to nascent peptides at rates of $10-20\ s^{-1}$ at 37 °C, and the chemical step of the peptide transfer reaction has a rate constant much bigger than that (e.g., ref *37*). In contrast, in the presence of saturating concentrations of substrates, the chemical step of the fragment reaction proceeds at rates around $0.01\ s^{-1}$ (*38*).

Large Subunit Function: Location of the Peptidyl Transferase Site. The location of the peptidyl transferase site was determined at low resolution by electron microscopy in 1995 (*19*, *20*). In the presence of mRNA, cognate peptidyl tRNAs and aminoacyl tRNAs bind side by side to the P and A sites of the 70S ribosome, respectively, with their CCA ends in the entrance of the exit tunnel in the large ribosomal subunit (see below). Since the CCA ends of tRNAs are the points of attachment of peptides and amino acids, when tRNAs bind to the ribosome this way, they must be in the peptidyl transferase site.

The position of the peptidyl transferase site has been determined crystallographically by solving the structures of the large subunit complexed with an A-site substrate analogue and with a peptidyl transferase transition state analogue (*34*). The A-site substrate analogue used is an RNA stem/loop, the stem sequence of which is that of the acceptor stem of tyrosyl tRNA, and its 3′-terminal sequence is CC-puromycin (Figure 1B). The transition state analogue employed was CCdA-P-puromycin, the so-called Yarus inhibitor (Figure 1C) (*39*). The phosphoramidite linking the dA to the tyrosyl group of the puromycin is tetrahedral and charged and thus mimics the tetrahedral intermediate generated when the α-amino group of an A-site-bound aminoacyl tRNA attacks the carbonyl carbon of the ester linking a nascent peptide to a tRNA in the P site.

There are many reasons for believing that these analogues bind to the peptidyl transferase site. First, the sites they occupy, which overlap, are at the small subunit end of the exit tunnel, as anticipated. Second, the terminal C of the CC-puromycin sequence of the A-site analogue pairs with G2588 in the A loop the way the corresponding C of A-site-bound tRNAs do (*40*). Third, the two Cs of the CCdA sequence of CCdA-P-puromycin pair with G2285 and G2284 in the so-called P loop, as the corresponding C's of P-site-bound tRNAs do (*41*). Fourth, if the binding of these analogues is physiologically relevant, their puromycin moieties ought to interact with the ribosome the same way, and they do. Fifth, there is preliminary data suggesting that peptide transfer occurs in these crystals when substrates having structures closely related to those of these analogues are soaked into them (M. Schmeing, personal communication). Finally, there is abundant evidence that the central loop of domain V in 23S rRNA is intimately involved in peptide transfer (*42*), and nucleotides from that part of 23S rRNA surrounds both analogues. In fact, there in nothing but domain V RNA anywhere in the immediate environment of both analogues.

The idea that the peptidyl transferase activity of the ribosome might be a manifestation of its RNA has a long history (*43*), and its credibility has risen as the body of data implicating RNA in ribosome function has grown relative to that implicating protein. Nevertheless, the existence of highly suggestive data notwithstanding (*44*), definitive proof of this proposition had never been obtained. The issue is now settled. All of the interactions between the two analogues and the ribosome involve rRNA. No protein atoms come close enough or could come close enough to the position identified by the phosphorus atom of the bound Yarus inhibitor to affect the chemistry that occurs there. The ribosome is a ribozyme.

Large Subunit Function: Sources of Catalytic Activity. Historically, it has always been much harder to determine the mechanism of enzymatic reactions than it has been to find out where they occur, and it is unlikely that the ribosome will be an exception to this rule. The task is made complicated in this instance because the state of the peptidyl transferase site the structure reveals relates to an activity that is qualitatively similar to the one of interest but that differs from it quantitatively.

No matter why the fragment reaction is so slow, the structures of the analogue/subunit complexes reveal one source of this enzyme's catalytic power. Peptide transfer is a bimolecular reaction, and all enzymes that promote bimolecular reactions bind their substrates so that the reactant atoms that must interact are appropriately juxtaposed. It is obvious that the ribosome does that much, and it cannot be excluded that this is *all* it does to accelerate the rate of peptide bond formation in vivo (*45*). Nevertheless, the structure suggests that it may do more.

In the CCdA-P-puro inhibitor/large subunit complex, the ribosome atom closest to the phosphorus atom of the inhibitor is A2486N3. It is about 3 Å from an oxygen of the phosphoramidite group, which is surprising because at the

pH of the crystal, ~6.0, both the oxygen and the nitrogen ought to be negatively charged. However, there is evidence that A2486 may have unusual properties. Strobel and colleagues (*46*) have shown that the reactivity of the corresponding base in the *E. coli* ribosome toward DMS titrates as though it were an acid having a pK_a of about 7.6. Since DMS can react with both AN1s and AN3s, this observation suggests that A2486N3 could have a pK_a around 7.5, instead of the normal pK_a of 1. If this were so, the proximity of that atom to the phosphoramidite oxygen would be easy to understand. At pH 6.0, A2486N3 will be protonated, and a protonated N3 can hydrogen bond with a phosphoramidite oxygen.

An adenine with a pK_a around 7.5 could promote peptide bond formation four different ways. First, it could deprotonate the α-amino groups of the A-site aminoacyl tRNAs. At pH 7.0, the α-amino groups of amino acids are protonated and positively charged, and they must be deprotonated during peptide bond formation because only neutral amino groups are nucleophiles. Second, it could act as a general base to remove a proton from the nitrogen of the (neutral) α-amino group of the attacking amino acid, as the new peptide bond is formed. Third, it could stabilize the tetrahedral intermediate by hydrogen bonding to it, which is the interaction visualized in the Yarus inhibitor structure. Fourth, it could donate its proton to the hydroxide anion formed as the deacylated tRNA is released from the tetrahedral intermediate.

The first possibility seems inconsistent with existing data. The pH dependence of the fragment reaction suggests the involvement of a base having a pK_a close to 7.5 in its rate-limiting step, A2486, for example. However, 50S subunits also catalyze the transfer of peptides from peptidyl tRNA to the hydroxyl groups of α-hydroxy puromycin derivatives, and the pH/rate profile for this reaction is the same as that of the fragment reaction (*47*). Since, at neutral pH, α-hydroxyl groups do not need to be deprotonated to function as nucleophiles, preliminary substrate deprotonation cannot be rate-limiting in either reaction.

The Yale group has proposed a model for the participation of A2486 in peptide bond formation that incorporates the remaining three elements (Figure 2). In it A2486 functions the same way in peptide transfer as the active site histidines do in serine proteases during the serine deacylation reaction. This proposal is being actively investigated in other laboratories, and we should learn a lot about the peptidyl transferase reaction soon.

Large Subunit Function: Anomalous pK_a of A2486. Whether A2486 helps to catalyze peptide formation or not, the evidence that it titrates anomalously is unambiguous, and it would be interesting to understand why. On this point too, the structure is suggestive. A2486 is positioned in the subunit by the base−base hydrogen bonds it forms with G2102 and G2482. G2482, in turn, forms an N3−O hydrogen bond with the phosphate group of A2485, which happens to be one of the least solvent-exposed phosphate groups in the entire subunit. There appear to be no metal ions bound in the neighborhood to help neutralize its charge. The Yale group has proposed that, acting though G2482, this phosphate group polarizes A2486, so that the version of its imino form that has a negative charge on N3 is favored (*34*). The similarity between this proposal and the charge-relay mechanism that has been invoked to explain the activity of serine proteases is obvious.

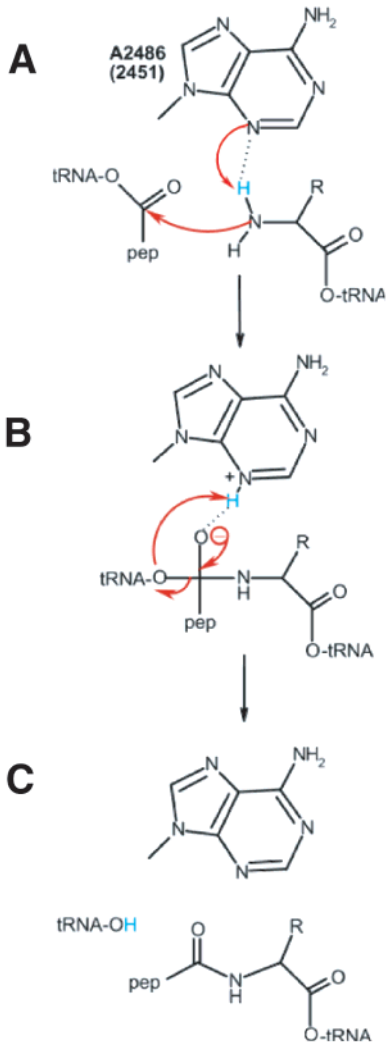

FIGURE 2: Mechanistic proposal for the involvement of A2486 (A2451 in *E. coli*) in the peptide transfer reaction. A2486 is shown in the imino tautomer believed to be favored by the local environment. (A) Abstraction of a proton from the attacking amino group. (B) Stabilization of the tetrahedral intermediate. (C) Protonation of the alkoxide of the leaving tRNA. (Figure adapted from ref *33*.)

Large Subunit Function: Peptide Exit Tunnel. The last aspect of large subunit function illuminated by its structure is the fate of nascent peptide chains. Nascent peptide chains first become exposed to solvent on the side of the large subunit opposite that which interacts with the small subunit (*48*), and there has long been evidence for a tunnel running from the peptidyl transferase site to that location (*49*, *50*). Any doubts there might have been about the existence of the exit tunnel were laid to rest by the intermediate resolution images of the ribosome published by electron microscopists in 1995 (*19*, *20*).

The crystal structure shows that the tunnel wall is mostly RNA but that, about 35 Å down from the peptidyl transferase site, its bore narrows because of the intrusion of peptide sequences belonging to proteins L4 and L22. Below that, it opens up again, and until the last 20 Å of its length or so, its wall remains entirely RNA. The RNA in the tunnel wall endows it with properties that are essential for its function. The wall has no large, hydrophobic patches on its surface,

nor are its hydophilic regions particularly large, and this reduces the likelihood of a nascent polypeptide binding to its surface so strongly that the tunnel would be blocked.

Two years ago, Brimacombe and co-workers did an elegant experiment that enabled them to identify the rRNA sequences adjacent to the N-termini of nascent polypeptides of different lengths (*51*). All of the sequences detected turn out to be components of the tunnel wall, and the longer the nascent peptide, the further down the tunnel they are located. At least some nascent peptides pass through the tunnel as they are synthesized!

Prospects for the Future. While it is exciting to be in possession of atomic coordinates for both subunits after all these years, it must be acknowledged that the elucidation of the molecular basis of protein synthesis has only just begun. Since many of the most difficult aspects of protein synthesis involve interactions between subunits, it is essential that an atomic resolution structure be obtained for the 70S ribosome, and happily one appears to be on its way, but we need much more. We need structures for the many other ribosomal intermediates that form during protein synthesis, and crystals exist for almost none of them.

The protein synthesis field has not become the exclusive preserve of the crystallographer. Electron microscopists have already contributed significantly to our understanding of the structures of many protein synthesis intermediates and doubtless will continue to do so (e.g., refs *52*−*54*). In addition, now that structures are available, site-directed mutagenesis experiments can be designed and interpreted with a precision that was previously unthinkable, and the same goes for the many techniques biochemists have devised for examining ribosome function in atomic detail. Finally, it is vital that the community that studies the kinetics of protein synthesis become reenergized. Only with their help will it become possible to understand the functional implications of the structure of the ribosome.

ACKNOWLEDGMENT

This review is an outgrowth of my longstanding collaboration with the other members of the Yale group that solved the structure of the large ribosomal subunit from *H. marismortui*, particularly Professor Thomas A. Steitz, Dr. Nenad Ban, Dr. Poul Nissen, and Dr. Jeffrey Hansen, and many of the thoughts it contains are products of my interactions with them. That said, responsibility for the opinions expressed here and whatever errors this review contains rests entirely with me.

REFERENCES

1. Garrett, R. A., Douthwaite, S. R., Liljas, A., Matheson, A. T., Moore, P. B., and Noller, H. F. (2000) *The Ribosome Structure, Function, Antibiotics and Cellular Interactions*, American Society for Microbiology, Washington, DC.
2. Tissieres, A. (1974) in *Ribosomes* (Nomura, M., Tissieres, A., and Lengyel, P., Eds.) pp 3−12, Cold Spring Harbor Laboratory, Cold Spring Harbor, NY.
3. Wittmann-Liebold, B. (1986) in *Structure, Function, and Genetics of Ribosomes* (Hardesty, B., and Kramer, G., Eds.) pp 326−361, Springer-Verlag, New York.
4. Moazed, D., and Noller, H. F. (1989) *Nature 342*, 142−148.
5. Byers, B. (1966) *J. Cell Biol. 30*, C1.
6. Clark, M. W., Hammons, M., Langer, J. A., and Lake, J. A. (1979) *J. Mol. Biol. 135*, 507−512.
7. Clark, M. W., Leonard, K., and Lake, J. A. (1982) *Science 216*, 999−1001.
8. Yonath, A., Mussig, J., Tesche, B., Lorenz, S., Erdmann, V. A., and Wittmann, H. G. (1980) *Biochem. Int. 1*, 428−435.
9. Trakanov, S. D., Yusupov, M. M., Agalarov, S. C., Garber, M. B., Rayazantsev, S. N., Tishenko, S. V., and Shirokov, V. A. (1987) *FEBS Lett. 220*, 319−322.
10. Yonath, A., Bennett, W., Weinstein, S., and Wittmann, H. G. (1990) in *The Ribosome. Structure, Function & Evolution* (Hill, W. E., Dahlberg, A., Garrett, R. A., Moore, P. B., Schlessinger, D., and Warner, J. R., Eds.) pp 134−147, American Society for Microbiology, Washington, DC.
11. Shevack, A., Gewitz, H. S., Hennemann, B., Yonath, A., and Wittmann, H. G. (1985) *FEBS Lett. 184*, 68−71.
12. van Bohlen, K., Makowski, I., Hansen, H. A. S., Bartels, H., Berkovitch-Yellen, Z., Zaytzev-Bushan, A., Meyer, S., Paulke, C., Francheschi, F., and Yonath, A. (1991) *J. Mol. Biol. 222*, 11−15.
13. Hope, H., Frolow, F., von Bohlen, K., Makowski, I., Kratky, C., Halfori, Y., Danz, H., Webster, P., Bartles, K. S., Wittmann, H. G., and Yonath, A. (1989) *Acta Crystallogr. B45*, 190−199.
14. Blundell, T. L., and Johnson, L. N. (1976) *Protein Crystallography*, Academic Press, London.
15. Ban, N., Freeborn, B., Nissen, P., Penczek, P., Grassucci, R. A., Sweet, R., Frank, J., Moore, P. B., and Steitz, T. A. (1998) *Cell 93*, 1105−1115.
16. O'Halloran, T. V., Lippard, S. J., Richmond, T. J., and Klug, A. (1987) *J. Mol. Biol. 194*, 705−712.
17. Andersson, I., Knight, S., Schneider, G., Lindqvist, Y., Lundqvist, T., Branden, C.-L., and Lorimer, G. H. (1989) *Nature 337*, 229−234.
18. Jack, A., Harrison, S. C., and Crowther, R. A. (1975) *J. Mol. Biol. 97*, 163−172.
19. Frank, J., Zhu, J., Penczek, P., Li, Y., Srivastava, S., Verschoor, A., Rademacher, M., Grassucci, R., Lata, R. K., and Agrawal, R. K. (1995) *Nature 376*, 441−444.
20. Stark, H., Mueller, F., Orlova, E. V., Schatz, M., Dube, P., Erdemir, T., Zemlin, F., Brimacombe, R., and van Heel, M. (1995) *Structure 3*, 815−821.
21. Ban, N., Nissen, P., Hansen, J., Capel, M., Moore, P. B., and Steitz, T. A. (1999) *Nature 400*, 841−847.
22. Clemons, W. M., Jr., May, J. L. C., Wimberly, B. T., McCutcheon, J. P., Capel, M. S., and Ramakrishnan, V. (1999) *Nature 400*, 833−840.
23. Cate, J. H., Yusupov, M. M., Yusupova, G. Z., Earnest, T. N., and Noller, H. F. (1999) *Science 285*, 2095−2104.
24. Tocilj, A., Schlunzen, F., Janell, D., Gluhmann, M., Hansen, H. A. S., Harmo, J., Bashan, A., Bartles, H., Agmon, I., Franceschi, F., and Yonath, A. (1999) *Proc. Natl. Acad. Sci. U.S.A. 96*, 14252−14257.
25. Ban, N., Nissen, P., Hansen, J., Moore, P. B., and Stetiz, T. A. (2000) *Science 289*, 905−920.
26. Wimberly, B. T., Brodersen, D. E., Clemons, W. M., Morgan-Warren, R. J., Carter, A. P., Vonrhein, C., Hartsch, T., and Ramakrishnan, V. (2000) *Nature 407*, 327−339.
27. Schluenzen, F., Tocilj, A., Zarivach, R., Harms, J., Gluehmann, M., Janell, D., Bashan, A., Bartles, H., Agmon, I., Franceschi, F., and Yonath, A. (2000) *Cell 102*, 615−623.
28. Gutell, R. R. (1996) in *Ribosomal RNA. Structure, Evolution, Processing and Function in Protein Biosynthesis* (Dahlberg, A., and Zimmerman, R., Eds.) pp 111−128, CRC Press, Boca Raton, FL.
29. Moore, P. B. (1999) *Annu. Rev. Biochem. 67*, 287−300.
30. Carter, A. P., Clemons, W. M., Brodersen, D. E., Morgan-Warren, R. J., Wimberly, B. T., and Ramakrishnan, V. (2000) *Nature 407*, 340−348.
31. Brodersen, D. E., Clemons, W. M., Carter, A. P., Morgan-Warren, R. J., Wimberly, B. T., and Ramakrishnan, V. (2000) *Cell 103*, 1143−1154.
32. Traut, R. R., and Monro, R. E. (1964) *J. Mol. Biol. 10*, 63.
33. Monro, R. E., and Marker, K. A. (1967) *J. Mol. Biol. 25*, 347.
34. Nissen, P., Ban, N., Hansen, J., Moore, P. B., and Stetiz, T. A. (2000) *Science 289*, 920−930.

35. Kjeldgaard, N. O., and Gaussing, K. (1974) in *Ribosomes* (Nomura, M., Tisseres, A., and Lengyel, P., Eds.) pp 369−392, Cold Spring Harbor Press, Cold Spring Harbor, NY.
36. Bilgin, N., Claesens, F., Pahverk, H., and Ehrenberg, M. (1992) *J. Mol. Biol. 224*, 1011−1027.
37. Pape, T., Wintermeyer, W., and Rodnina, M. V. (1998) *EMBO J. 17*, 7490−7494.
38. Maden, B. E. H., Traut, R. R., and Monro, R. E. (1968) *J. Mol. Biol. 35*, 333−345.
39. Welch, M., Chastang, J., and Yarus, M. (1995) *Biochemistry 34*, 385−390.
40. Kim, D. F., and Green, R. (1999) *Mol. Cell 4*, 859−864.
41. Samaha, R. R., Green, R., and Noller, H. F. (1995) *Nature 377*, 309−314.
42. Noller, H. F. (1984) *Annu. Rev. Biochem. 53*, *119−162*.
43. Crick, F. H. C. (1968) *J. Mol. Biol. 38*, 367−379.
44. Noller, H. F., Hoffarth, V., and Zimniak, L. (1992) *Science 256*, 1416−1419.
45. Nierhaus, K. H., Schulze, H., and Cooperman, B. S. (1980) *Biochem. Int. 1*, 185−192.
46. Muth, G. W., Ortoleva-Donnelly, L., and Strobel, S. A. (2000) *Science 289*, 947−950.
47. Fahnestock, S., Neumann, H., Shahoua, V., and Rich, A. (1970) *Biochemistry 9*, 2477−2483.
48. Bernabeu, C., and Lake, J. A. (1982) *Proc. Natl. Acad. Sci. U.S.A. 79*, 3111−3115.
49. Milligan, R. A., and Unwin, P. N. T. (1986) *Nature 319*, 693−695.
50. Yonath, A., Leonard, K. R., and Wittmann, H. G. (1987) *Science 236*, 813−816.
51. Choi, K. M., and Brimacombe, R. (1998) *Nucleic Acids Res. 26*, 887−895.
52. Agrawal, R. K., Spahn, C. M. T., Penczek, P., Grassucci, R., Nierhaus, K. H., and Frank, J. (2000) *J. Cell Biol. 150*, 447−459.
53. Stark, H., Rodnina, M. V., Wieden, H.-J., van Heel, M., and Wintermeyer, W. (2000) *Cell 100*, 301−309.
54. Agrawal, R. K., Heagle, A. B., Penczek, P., Grassucci, R. A., and Frank, J. (1999) *Nat. Struct. Biol. 6*, 643−647.

BI0029402